ORIGINAL RESEARCH PAPER

Resveratrol alleviates vascular inflammatory injury by inhibiting inflammasome activation in rats with hypercholesterolemia and vitamin D2 treatment

Zu Yue Deng[1,2] · Meng Mei Hu[1,2] · Yan Fei Xin[3] · Chen Gang[3]

Abstract

Objective Atherosclerosis (AS) is an inflammatory disease involved in vascular inflammatory injury. The inflammasome is an important part of inflammatory diseases and participates in the vascular inflammatory injury. Resveratrol (RSV) possesses anti-inflammatory activities, but its effects on inflammasomes during vascular injury remain unclear. This study focused on the effects and mechanisms of RSV on inflammasomes during vascular injury.

Methods Male Sprague–Dawley rats were treated with a purified diet or cholesterol-enriched diet combined with vitamin D2 (VD; 1.8 million units/kg/days, Po) and saline or RSV (50 mg/kg/days, Po) daily for 5 weeks. The concentrations and enzyme activities of related indicators were measured by a spectrophotometer or ELISA kit. Their gene and protein expression levels were analyzed by reverse transcription–polymerase chain reaction and Western blot, respectively.

Results Upon administration with RSV, rats with combined hyper cholesterol and VD demonstrated the following changes: the vascular histopathological changes were relieved, and the level of the von Willebrand factor decreased. The level of serum IL-1β, a marker of inflammasome activation, significantly decreased. The mRNA and protein expression levels of the three components of inflammasomes, namely, NOD-like receptor pyrin domain containing 3, apoptosis-associated speck-like protein containing a caspase-recruitment domain, and caspase-1, were downregulated. The effects of RSV were closely related to hypolipidemia (decrease in the levels of total cholesterol, triglycerides, and low-density lipoprotein cholesterol combined with the expression of the lectin-like ox-LDL receptor and increase in high-density lipoprotein cholesterol), antioxidation (decrease in MDA levels and increase in SOD and GPx activities), and anti-inflammation (downregulation of the expression of IL-1β, intracellular adhesion molecule-1, and monocyte chemotactic protein-1). The mechanisms for the downregulation of NF-κB p65 and p38 MAPK expression, as well as the upregulation of SIRT1 expression, were analyzed.

Conclusion This study proved that RSV inhibited inflammasome activation to protect vascular injury in vivo. RSV exhibited therapeutic potential in the treatment of vascular injury.

Responsible Editor: Bernhard Gibbs.

✉ Zu Yue Deng
dzy7317@sina.com

1   Zhejiang University of Technology, Hangzhou 310004, Zhejiang, China

2   Zhejiang Institute for Food and Drug Control, Hangzhou, Zhejiang, China

3   State Key Laboratory of Safety Evaluation for New Drug, Zhejiang Academy of Medical Sciences, Hangzhou, Zhejiang, China

Introduction

Lipid metabolism disorder has long been considered the main cause of atherosclerosis (AS). Ross and Glomset [1, 2] proposed the theory of endothelial injury and later added

the concept of response to injury [3, 4]. The injury is often closely related to the level of inflammation; thus, inflammation plays an important role in AS [5]. The inflammasome is a relatively new discovery in immunology, and this complex has attracted widespread attention in inflammation research [6]. The NOD-like receptor pyrin domain containing 3 (NLRP3) is the most well-characterized inflammasome [7]. The activation of the NLRP3 inflammasome can produce the pro-inflammation cytokine IL-1β, which increases the expression of vascular cell adhesion molecule-1, intercellular adhesion molecule-1 (ICAM-1), and monocyte chemotactic protein (MCP) [8]. These cytokines can cause vascular injury and AS formation. Some studies [9–11] also found that the inflammasome and IL-1β are contributors of several common human diseases, such as gout, type II diabetes, nonalcoholic steatohepatitis, AS, Alzheimer's disease, and cancer.

The process of NLRP3 inflammasome activation that leads to the release of IL-1β is complex. Divergent invading pathogens and cellular damage result in the assembly and activation of NLRP3, the apoptosis-associated speck-like protein containing a caspase-recruitment domain (ASC), and caspase-1 into multi-molecular platforms (NLRP3 inflammasomes). These activated NLRP3 inflammasomes mediate the catalytic activation of caspase-1, which is followed by the cleavage and release of the pro-inflammatory cytokines IL-1β and IL-18 [7].

Resveratrol (3,5,4-trihydroxystilbene, RSV) is a plant-derived polyphenol present in grapes and red wine. This compound possesses antioxidant, anti-aging, anti-inflammatory, anti-carcinogenic, cardioprotective, anti-proliferative, and immunomodulatory properties [12]. Dong et al. [13] reported that RSV inhibits foam cell formation by regulating the expression of MCP-1 and activating the AMP-activated protein kinase (AMPK)—Sirtuin 1 (SIRT1)—peroxisome proliferator-activated receptor (PPAR) signaling pathway. cis-RSV produces anti-inflammatory effects by inhibiting the canonical and non-canonical inflammasomes in macrophages [14]. SIRT1 enhanced by RSV exerts anti-inflammatory effects by regulating NLRP3 expression partially through the NF-κB pathway in mesenchymal stem cells [15]. In vitro experiments have shown the effects of RSV on the NLRP3 inflammasome, as well as the mechanisms involved. We hypothesize that RSV has similar effects in vivo. To confirm this hypothesis, we established a hyperlipidemia model in rats treated with a cholesterol-enriched diet combined with vitamin D2 (VD). The effects of the inflammasome in vascular injury in model rats and RSV on vascular NLRP3 inflammasome activation were also investigated. In this model, hyperlipidemia initiates vascular injury, whereas VD aggravates the injury. VD induces the

deposition of calcium in the vascular wall [16]. Increased cytoplasmic Ca^{2+} promotes the assembly of inflammasome components, and intracellular Ca^{2+} is required for spontaneous inflammasome activity [17]. Hypercholesterolemia might accelerate vascular calcification by ox-LDL [18]. Calcifying VSMCs upregulated the mRNA expression of the Nalp3 inflammasome complex, including Nalp3, ASC, and caspase-1 [17].

Our results showed that RSV decreased vascular injury and protected vascular function by inhibiting inflammasome activation. The effects were closely related to hypolipidemia, antioxidation, and anti-inflammation. This mechanism involved the upregulation of SIRT1 and downregulation of NF-κB p65 and p38 MAPK expression.

Materials and methods

Animals and experimental design

Five-week-old male Sprague–Dawley rats [Certificate No. SCXK(hu)2012-0002] (180 ± 25 g) were purchased from the Shanghai Slrc Laboratory Animal Company Limited (Shanghai, China). All experiments were approved by the laboratory animals ethical committee of the Zhejiang Provincial Research Institute for Food and Drug Control, following the NIH guide for laboratory animals (NIH Publication No. 80-23, revised 1978) for the care and use of animals. The rats were individually housed under laboratory conditions (room temperature of 20 ± 3 °C, humidity of 60 ± 10 %, and a 12 h light–dark cycle), and water was provided ad libitum. After 1 week of acclimatization, the animals were randomly divided into four groups (with ten animals per group): the normal control group (NC), RSV control group (RSV), hypercholesterolemia combined with VD (Sigma, USA) group (HC+VD), and RSV (Hangzhou Lin'an Tianhong Bio-tech Co., Ltd.) treatment group (RSV+HC+VD). Rats from the NC and RSV groups were fed a standard diet, and the other two groups were fed a cholesterol-enriched diet combined with VD [a standard laboratory diet supplemented with cholesterol (2 %), lard (3 %), cholic acid (0.5 %), and propylthiouracil (0.2 %)] plus oral administration of a high dose of VD (1.8 million uayd) for 5 weeks. RSV was administered orally (50 mg/kg body weight/day in 20 % ethanol solution in the RSV and HC+RSV+VD groups) by an orogastric catheter for 5 weeks. The same volume of distilled water was given orally in rats in the NC and HC groups. RSV was prepared and provided daily. The body weight was measured every week for 6 weeks. The general condition of the experimental animals was observed every day. The dosage of RSV used was based on the literature [8] and our previous study.

Sample collection of blood and thoracic aorta tissue

After 5 weeks of treatment, rats were fasted for 12 h and then sacrificed. Blood samples were collected from the abdominal aorta, and serum was separated by centrifugation at 4 °C and stored at −20 °C for biochemical analysis. Arteries from individual rats were used for histological, gene expression, and Western blot analyses.

Serum biochemical analysis

Levels of serum total cholesterol (TC), triglyceride (TG), low-density-lipoprotein cholesterol (LDL-C), high-density-lipoprotein cholesterol (HDL-C), and C-reactive protein (CRP) were measured using a Hitachi 7020 automatic analyzer and kits obtained from Shanghai Shenergy-Diasys Diagnostics Technology Co. Ltd.

Determination of superoxide dismutase (SOD) activity, glutathione peroxidase (GPx) activity, malondialdehyde (MDA) levels, and the von Willebrand factor (vWF) in serum

SOD activity, GPx activity, MDA level, and vWF level in serum were measured using kits (Jiancheng, China), namely, the MDA assay kit (TBA method), SOD assay kit (hydroxylamine method), GSH-PX assay kit (colorimetric method), and vWF kit (ELISA), respectively. The concentrations of IL-1β and TNF-α were determined in aqueous samples by ELISA kits (R&D Systems, Minneapolis, MN, USA). All protocols were performed according to the manufacturer's instructions.

RNA extraction and quantitative real-time polymerase chain reaction (PCR)

The relative mRNA levels of control GAPDH were determined by real-time PCR. Total RNA was extracted from frozen-stored artery from different rat groups using TRizol reagent (Takara, Dalian, China). cDNA synthesis was performed by MuLVReverse Transcriptase (Takara, Dalian, China). Real-time PCR was performed using a SYBR Green PCR master mix kit (Roche, USA). The primer sequences were designed according to the GenBank database using Beacon Designer software (Premier Biosoft). The primer sequences are listed in Supplemental Table 1. PCR reactions were performed at 95 °C for 30 s and subjected to 40 cycles of 95 °C for 10 s, 55 °C for 10 s, and 72 °C for 30 s. These reactions were performed in triplicate for each sample primer set, and the mean of the three experiments was used as the relative quantification value. At the end point of each PCR cycle, melting curves were generated to assess product purity. Data were analyzed with Roche-gene software (Roche, USA). The relative levels of each gene expression were determined by the $2^{-\Delta\Delta Ct}$ method.

Western blot

Thoracic aorta samples (0.5 g) were homogenized in 1 mL of RIPA lysis buffer (Beyotime Institute of Biotechnology, China) containing the Protease Inhibitor Cocktail set III (Beyotime). Tissue lysates were incubated on ice for 30 min and centrifuged at $12,000 \times g$ at 4 °C for 20 min. The supernatant was collected, and protein concentrations were measured by a Coomassie blue staining kit (Beyotime) using BSA as a standard. Samples containing 100 μg of protein were separated by 10 or 15 % sodium dodecyl sulfate PAGE, and then, the proteins were electrotransferred onto a nitrocellulose membrane. The membranes were washed in Tris–Tween buffered saline [TTBS, 20 mmol/L Tris–HCl buffer, pH 7.5, containing 150 mmol/L NaCl and 0.05 % (v/v) Tween 20] and incubated with primary antibodies anti-caspase-1(45 kDa) Mouse monoclonal antibody (1:500 dilution) and rabbit polyclonal IgG anti-rat lectin-like oxidized LDL receptor-1 (LOX-1) (Bioss, China, 50 kDa), NLRP3 (106 kDa), ASC (24 kDa), Caspase-1(45 kDa), IL-1β (37 kDa), IL-18 (18 kDa), MCP-1(12 kDa), ICAM-1(90 kDa) NF-κB p65 (60 kDa), p38 MAPK(42 kDa), p-p38 MAPK (38 kDa) and SIRT1 (120 kDa) (Santa Cruz, USA), and GAPDH (37 kDa) (Beyotime) (1:500 dilution) in diluent buffer [5 % (w/v) BSA and 0.1 % Tween 20 in TBS] overnight at 4 °C followed by blocking with 5 % skimmed milk in TTBS 1 h at room temperature with gentle agitation. Membranes were incubated with a 1:1000 dilution (v/v) of secondary antibody, goat anti-mouse, and anti-rabbit IgG-HRP conjugate (Beyotime) after washing three times in TTBS. Membranes were washed in TTBS three times. Protein bands were developed using an HRP system (Beyotime). Protein bands were visualized by enhanced chemiluminescence using a BeyoECL Plus Kit (Beyotime), and images were displayed with Kodak X-Omat BT film (5 in. ×7 in.; Beyotime). Band intensity was quantified with Gel-Pro Analyzer software (Liu Yi, Beijing). GADPH was used as a loading control.

Histological examinations

For histopathological analysis, thoracic aorta segments were dissected and fixed in 10 % neutral buffered formalin. These segments were subsequently embedded in paraffin and sectioned at 6-μm thickness with a slicing machine (Leica RM2265; Germany). The sections were stained with hematoxylin and eosin and then imaged using a microscope

(Leica DM4000 BLED; Germany) for histological examination.

Immunohistochemical assay

Protein expression was immunohistochemically detected via the streptavidin–peroxidase conjugated method. In the thoracic aorta sections, endogenous peroxidase activity was inactivated with 3 % H_2O_2 for 10 min. The sections were incubated with primary antibodies against NLRP3, ASC, IL-1β, IL-18, and caspase-1 (Santa Cruz, USA) overnight at 4 °C. The sections were thoroughly washed in PBS the following day and incubated with goat anti-rabbit bi-otinylated secondary antibody IgGs (Beijing Zhongshan, China) followed by HRP-conjugated streptavidin. The sections were stained with diaminobenzidine (Zhongshan, China). Negative controls were obtained by replacing specific antisera with PBS. Antibody binding was visualized and photographed under light microscopy. An Image-Pro Plus image analysis system was used for densitometric quantification of the positive VWF-, NLRP3-, ASC-, caspase-1-, IL-1β-, and IL-18-expressing cells.

Statistical analysis

Data are expressed as the mean ± standard deviation. The values were calculated from the specified number of determinations with SPSS statistical software package (version 17.0; SPSS, Chicago, IL, USA). Significant differences between the experimental and control groups were assessed by the Student's t test (two-experimental group data analysis) and one-way ANOVA (multi-experimental group data analysis). $P < 0.05$ was considered statistically significant.

Results

Serum lipid metabolism

No significant differences in the serum levels of TC, LDL-C, and HDL-C were observed between the RSV and NC groups, thereby suggesting that treatment with RSV alone did not affect normal serum lipid levels. However, compared with the NC group, the TG, TC, and LDL-C levels in the HC+VD group were significantly elevated (1.8-, 1.9-, and 1.3-fold, respectively; $P < 0.01$ or $P < 0.05$), whereas the levels of HDL-C decreased (17 %, $P < 0.05$). Compared with the HC+VD group, RSV treatment significantly reduced the levels of TG, TC, and LDL-C (33, 48, and 27 %, respectively; $P < 0.01$ or $P < 0.05$), but increased the levels of HDL-C (1.3-fold, $P < 0.05$) in the RSV+HC+VD group (Fig. 1).
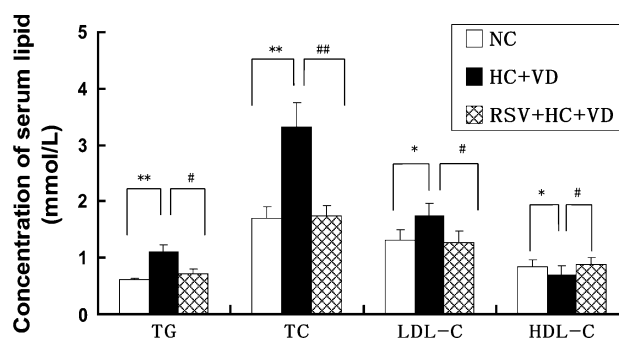

Fig. 1 Effects of RSV on lipid metabolism. Experimental rats were fed with a hypercholesterol diet combined with vitamin D2 and then treated with the solvent or with RSV. The amounts of TG (**a**), TC (**b**), LDL-C (**c**), and HDL-C (**d**) in the blood samples were determined. Data are expressed as the TG, TC, LDL-C, and HDL-C content (mean ± SEM, $n = 10$). *$P < 0.05$, **$P < 0.01$, compared with NC rats; #$P < 0.05$, ##$P < 0.01$, compared with HC+VD rats

Lipid peroxidation and antioxidant enzyme levels

To study the function of RSV on antioxidant activity, we determined different oxidation indices. Compared with the NC group, RSV treatment did not significantly influence SOD and GPx activity nor did it decrease the MDA content. The HC+VD group demonstrated a 1.7-fold elevation in the MDA content ($P < 0.01$) but exhibited decreased SOD and GPx activity (63 and 24 %, respectively; $P < 0.01$ or $P < 0.05$) in serum. Compared with the HC+VD group, the RSV+HC+VD group had a significant decrease in the MDA content (37 %, $P < 0.05$), as well as increased SOD (2.4-fold, $P < 0.01$) and GPx activity (1.4-fold, $P < 0.05$) in serum (Fig. 2).

RSV ameliorated hypercholesterolemia combined with VD-induced vascular injury

Hypercholesterolemia causes vascular endothelial injury, and VD aggravates this injury by depositing excessive calcium in the vessel [16]. vWF is a well-known marker of endothelial function/injury [19]. Compared with the normal rats, no differences in the serum vWF levels and vascular histopathological changes in the RSV group were observed (Figs. 3, 4). However, the vWF concentrations in serum increased by 2-fold ($P < 0.01$; Fig. 3e) and vWF expression in the vascular endothelium (immunohistochemistry) increased by 2.5-fold ($P < 0.01$) in the HC rats (Fig. 3c, f). Compared with the HC+VD group, RSV treatment significantly reduced the vWF levels (45 %; $P < 0.05$) and vWF expression (39 %; $P < 0.05$) in the RSV+HC+VD rats (Fig. 3d, f). As shown in (Fig. 4a–d), morphological examination of the aorta sections showed the pathomorphometrical characteristics of AS. Compared with the normal rats, the HC rats had aortas with disordered
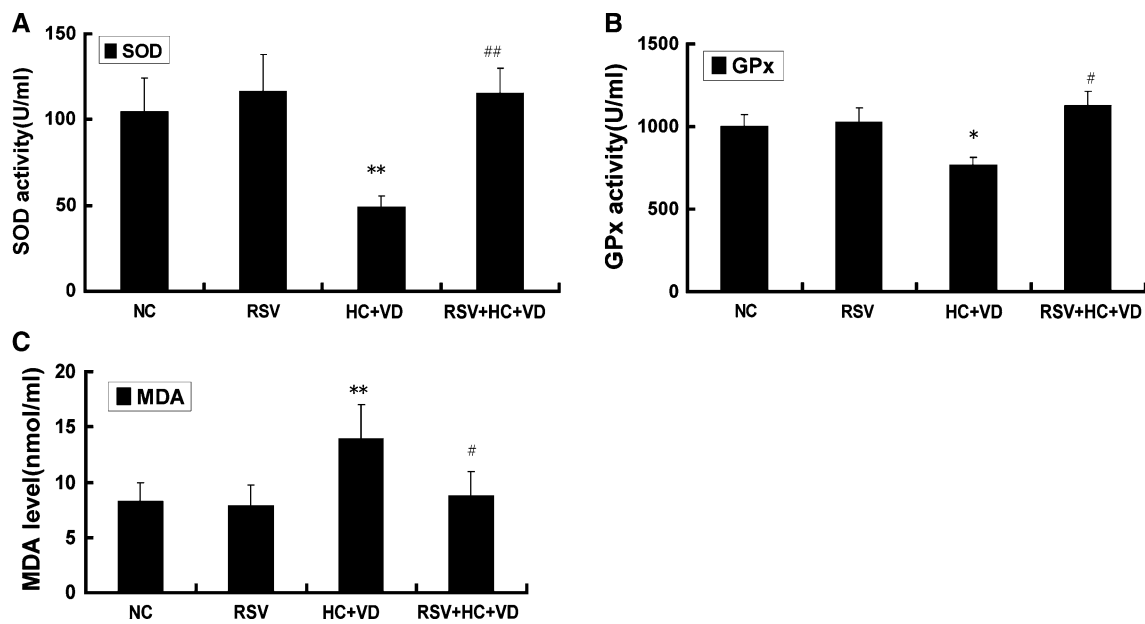
Fig. 2 Antioxidative effects of RSV on lipid peroxidation and SOD and GPx activity. Experimental rats were fed with a hypercholesterol diet combined with vitamin D2 and then treated with the solvent or with RSV. SOD (**a**) and GPx (**b**) activity, as well as the MDA content (lipid peroxidation, **c**), in the blood samples were determined. Data are expressed as the MDA content or activity of SOD or GPx (mean ± SEM, $n = 10$). $*P < 0.05$, $**P < 0.01$, compared with NC rats; $^{\#}P < 0.05$, $^{\#\#}P < 0.01$, compared with HC+VD rats
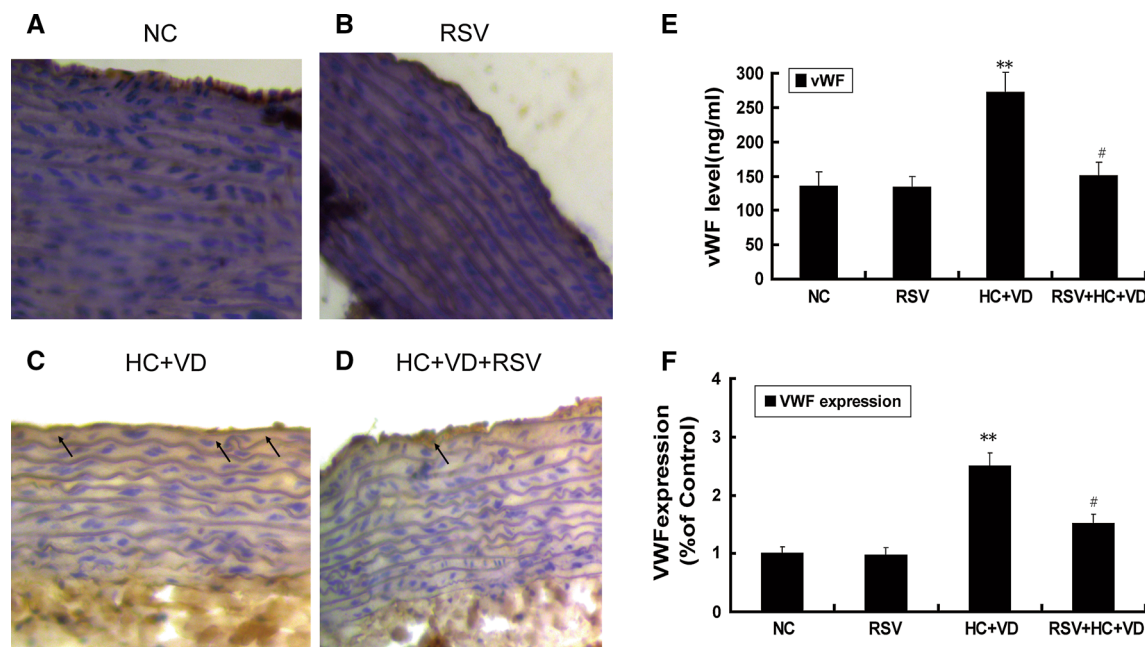

Fig. 3 Expression of vWF in the vascular endothelium of rats (immunohistochemistry; SP, original magnification ×400). The serum levels of **a** NC, **b** RSV, **c** HC+VD, **d** RSV+HC+VD, and **e** a marker of endothelial injury called vWF were measured in four groups ($n = 10$). **f** vWF expression was observed by immunohistochemical studies in the aorta in four groups ($n = 10$). Administration of RSV obviously reduced the levels and expression of vWF. The *brown arrows* indicate immunoreactivity. The intensity was calculated by Image-Pro Plus software. Data are expressed as the mean ± SEM of every ten individual experiments. $*P < 0.05$, $**P < 0.01$, compared with NC rats; $^{\#}P < 0.05$, $^{\#\#}P < 0.01$, compared with HC+VD rats (color figure online)

arrangement, unclear borderlines, and partial deletion, as well as increased foam cell formation (3.4-fold; $P < 0.01$) and tunica media thickness of the vascular walls (2.1-fold;

$P < 0.01$; Fig. 4c, e). Compared with the HC+VD group, RSV administration attenuated the vascular histopathological changes, such as decreased foam cell formation
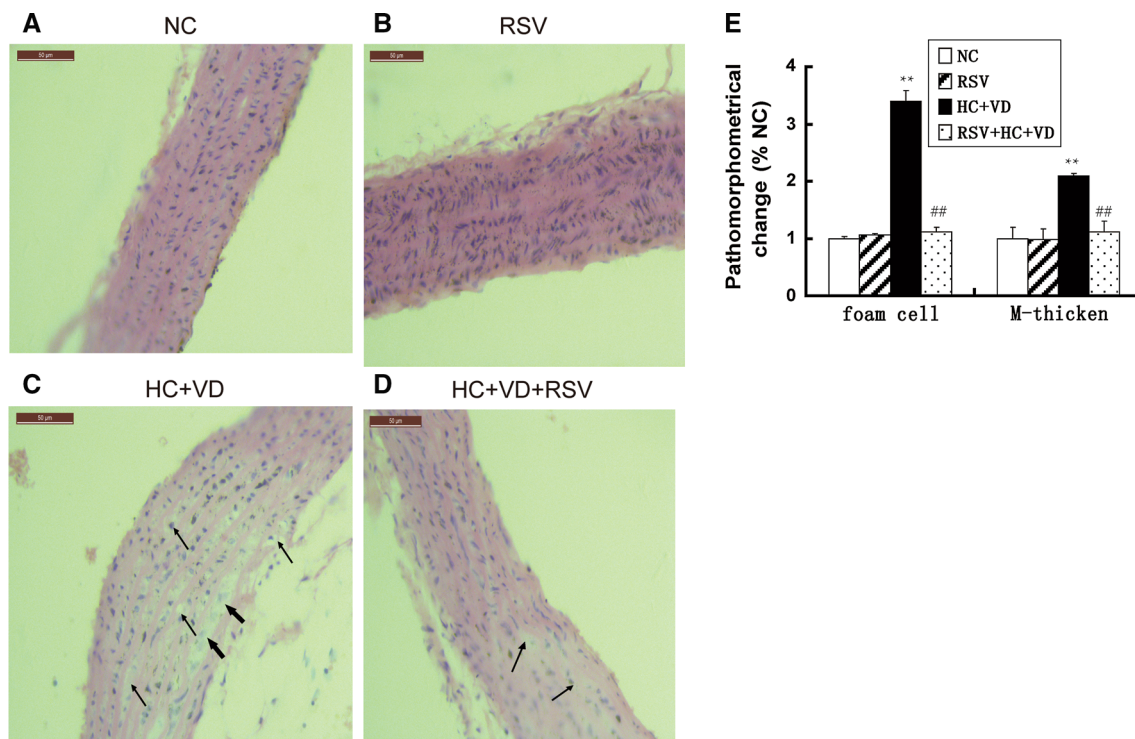
Fig. 4 RSV reduced vascular injury. **a** Normal histology of the thoracic aorta was observed in the NC group. The pathomorphometrical characteristics of atherosclerosis, including disordered arrangement, unclear borderline, partial deletion, formation of foam cells and cholesterol crystals, and tunica media thickening of vascular walls, were observed in the HC+VD group (**c**). **d** Administration with RSV obviously reduced the vascular histopathological changes in the RSV+HC+VD group (hematoxylin and eosin staining, ×200). *Thin arrows* indicate the foam cells, and *bold arrows* indicate cholesterol crystals. **e** Pathomorphometrical changes, including the number of foam cells and thickness of the tunica media in the aorta. Five fields of vision were selected to count the number of foam cells in individual experiments (×200). Results are expressed as the mean ± SEM of every experiment with ten individuals each. Image-Pro Plus software was used to calculate the ring diameter of the inner and external elastic membrane (×50). The thickness of tunica media = (the ring diameter of external elastic membrane − the ring diameter of inner elastic membrane)/2π. Results are expressed as the mean ± SEM of ten individuals in each experiment. *$P < 0.05$, **$P < 0.01$, compared with NC rats; #$P < 0.05$, ##$P < 0.01$, compared with HC+VD rats

67 % ($P < 0.01$) and tunica media thickness 47 % ($P < 0.05$), in the aorta in the RSV+HC+VD group (Fig. 4d, e).

RSV decreased the levels of inflammatory cytokines in rats with combined hypercholesterolemia and VD

To identify the effects of RSV on inflammatory cytokines, we detected the serum levels of these cytokines. Compared with the NC group, the RSV group did not significantly influence the NF-α, IL-1β, and CRP levels (Fig. 5a–c). The IL-1β levels in the HC+VD group were greatly enhanced (1.8-fold, $P < 0.01$), but the levels of TNF-α and CRP did not significantly change (Fig. 5a, c). However, compared with the HC+VD group, RSV treatment significantly reduced IL-1β production in the RSV+HC+VD group (43 %, $P < 0.05$). All these results suggested that RSV could decrease the IL-1β levels (Fig. 5b).

RSV inhibited the activation of NLRP3 inflammasome

To identify the effects of RSV on the NLRP3 inflammasome, we examined the expression levels of NLRP3, ASC, caspase-1, and IL-1β by real-time RT-PCR (Fig. 6b) and Western blot analysis (Fig. 6a). Compared with the NC group, the group with RSV alone slightly reduced the mRNA (43 %, $P < 0.05$) and protein (32 %, $P < 0.05$) expression levels of IL-1β. Hypercholesterol combined with VD rats could increase the mRNA (5.6-, 6.9-, 4.3-, and 5.2-fold, respectively; $P < 0.01$) and protein (3.6-, 3.7-, 1.3-, and 2.5-fold, respectively; $P < 0.01$) expression levels of NLRP3, ASC, caspase-1, and IL-1β. However, compared with the HC+VD group, RSV pretreatment (50 mg/kg/d) downregulated the mRNA (65, 68, 45, and 52 %; $P < 0.01$) and protein (63, 79, 35, and 39 %; $P < 0.01$ or $P < 0.05$) expression of NLRP3, ASC, caspase-1, and IL-1β, respectively, in the RSV+HC+VD group. No significant
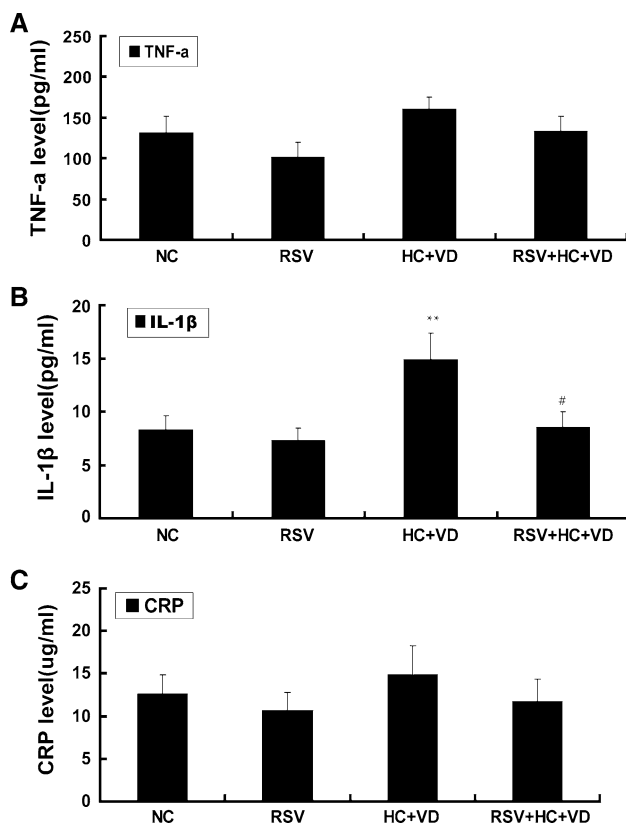
Fig. 5 RSV decreased the production of pro-inflammatory cytokines in rats with combined hypercholesterolemia and VD. **a** ELISA assays of tumor necrosis factor-alpha (TNF-α) **b** and interleukin-1 beta (IL-1β). **c** CRP was detected by an automatic analyzer. Results are expressed as the mean ± SEM of every ten individual experiments. $*P < 0.05$, $**P < 0.01$, compared with NC rats; $^{\#}P < 0.05$, $^{\#\#}P < 0.01$, compared with HC+VD rats

difference was found in the mRNA and protein expression of IL-18. These results were also confirmed by immunohistochemical examination (Fig. 7), which indicated that RSV could prevent the noted increases in several parameters in vascular injury molecules, including NLRP3, ASC, caspase-1, and IL-1β, in rats with combined hypercholesterolemia and VD. Thus, RSV could inhibit inflammasome activation and ameliorate hypercholesterol combined with the VD-induced production of IL-1β.

Effects of RSV on the expression of LOX-1, ICAM-1, MCP-1, NF-κB p65, p38 MAPK, and SIRT1 in the thoracic artery of rats

Hypercholesterolemia secretes inflammatory mediators, including cytokines, adhesion molecules, lipid mediators of inflammation, and reactive oxygen metabolites. Given that RSV inhibited the release of pro-inflammatory cytokines in rats with hypercholesterolemia, we investigated the effects of RSV on adhesion molecules, lipid mediators, and the related signaling pathways. The mRNA

and protein expression levels of LOX-1, MCP-1, ICAM-1, NF-κB p65, p38 MAPK, and SIRT1 were examined. Compared with the normal rats, RSV treatment increased the mRNA and protein expression levels of SIRT1 (2.6-, and 1.5-fold, respectively; $P < 0.01$). However, no significant differences were observed between the RSV and NC groups in terms of the other indices. The HC+VD group demonstrated significantly upregulated mRNA expression of LOX-1, MCP-1, ICAM-1, NF-κB p65, and p38 MAPK (4.6-, 5.8-, 6.1-, 3.2-, and 1.4-fold, respectively; $P < 0.01$ or $P < 0.05$) and protein expression of LOX-1, MCP-1, ICAM-1, NF-κB p65, and p-p38 MAPK (2.5-, 3-, 3.1-, 2.2-, and 3.6-fold, respectively; $P < 0.01$), as well as downregulated mRNA (34 %; $P < 0.05$) and protein (15 %) expression of SIRT1 in the thoracic aorta. Compared with the HC+VD group, RSV treatment (50 mg/kg) remarkably decreased the mRNA expression of LOX-1, MCP-1, ICAM-1, NF-κB p65, and p38 MAPK by 77, 64, 66, 66, and 31 %, respectively ($P < 0.01$ or $P < 0.05$), and protein expression of LOX-1, MCP-1, ICAM-1, NF-κB p65, and p-P38 MAPK by 63, 54, 53, 59, and 60 %, respectively ($P < 0.01$), and upregulated the mRNA (3.2-fold; $P < 0.01$) and protein (1.7-fold; $P < 0.01$) expression of SIRT1 in the RSV+HC+VD rats. Therefore, RSV could decrease vascular injury molecules in rats with combined hypercholesterolemia and VD (Fig. 8).

Discussion

The combination of hypercholesterolemia and VD in the present research caused the following pathomorphometrical changes in rat aortas: disordered arrangement, unclear borderline, partial deletion, foam cell formation, and tunica media thickening in the vascular walls. The results showed that the combination of hypercholesterolemia and VD caused vascular injury. Vascular injury often involves many inflammatory mediators, such as TNF-α and IL-1β. These pro-inflammatory cytokines promote monocyte macrophages and vascular endothelial cells to synthesize various cytokines, adhesion molecules, and acute phase proteins, such as IL-2, IL-6, and CRP [20]. IL-1β is also tightly regulated by the NLRP3 inflammasome cascade [21]. Previous studies found that RSV reduces inflammatory mediators by various mechanisms [22, 23]. RSV can partially regulate NLRP3 expression through the NF-κB pathway or AMPK–SIRT1–PPAR signaling pathway [13–15]. However, these results were mainly from cell culture experiments, and whether RSV has similar effects in vivo remains unclear. The present study investigated the effects of RSV on inflammasome activation and its mechanism in the vascular injury of rats. Our study showed that RSV

Fig. 6 RSV suppressed inflammasome activation and production of IL-1β induced by hyper cholesterol combined with VD. **a** Thoracic aorta samples were processed for the extraction of total protein. Western blot analyses of NLRP3, ASC, and caspase-1 were used to study the maturation of IL-1β and IL-18. GAPDH (w37 kDa) was used to control equal loading. **b** Total RNA from the thoracic artery of experimental rats and the mRNA expression of NLRP3, ASC, and caspase-1, as well as maturation of IL-1β and IL-18, were determined by real-time RT-PCR. GAPDH was used as a standard housekeeping gene. Results are expressed as the mean ± SEM of three individual experiments. *$P < 0.05$, **$P < 0.01$, compared with NC rats; #$P < 0.05$, ##$P < 0.01$, compared with HC rats
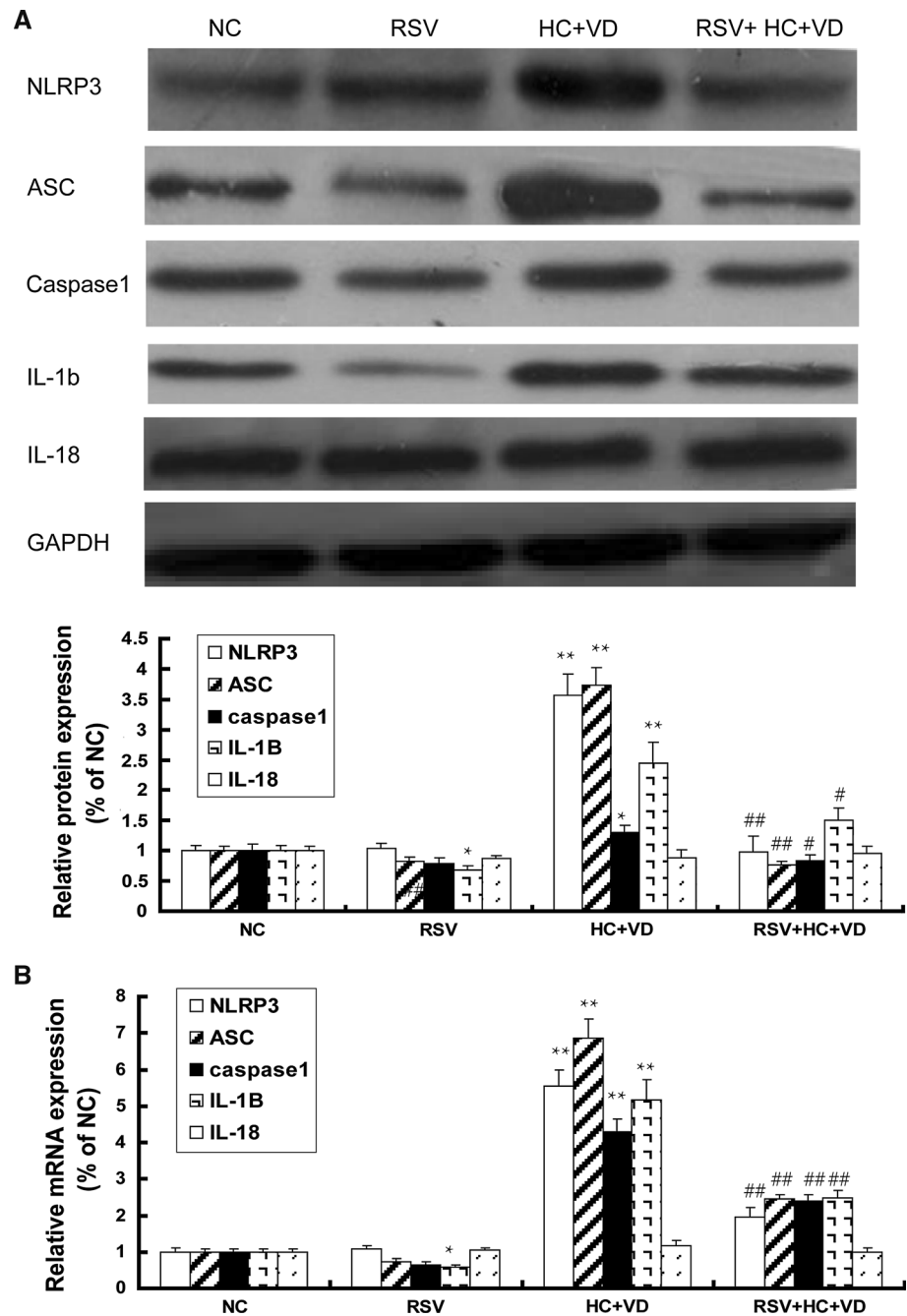
downregulated the mRNA and protein expression of NLRP3, ASC, caspase-1, and IL-1β in hypercholesterolemia and VD rats. The results demonstrated that RSV ameliorated IL-1β production by inhibiting the expression of NLRP3 inflammasome, and this process involved numerous factors.

Cholesterol crystals in AS activate the inflammasomes, thereby resulting in IL-1β production [24]. TC and ox-LDL are involved in the formation of cholesterol crystals. In hypercholesterolemia, higher TC and LDL were observed. Our previous report demonstrated that LDL, VLDL, and HDL are oxidized in vivo in hypertriglyceridemia patients [25]. ox-LDL can recognize and upregulate LOX-1 in endothelial cells, macrophages, and vascular smooth muscle cells. TC, especially oxidative TC, which was loaded by ox-LDL, was deposited in cells to facilitate the formation of cholesterol crystals. LOX-1 and LDLR can affect the synthesis of pro-inflammatory and pro-oxidative products, such as the NF-κB signaling pathways (presence of activity change) [26]. We found that RSV decreased the TC and LDL-C levels in serum and LOX-1 expression in hypercholesterolemia and VD rats. Thus, RSV could reduce
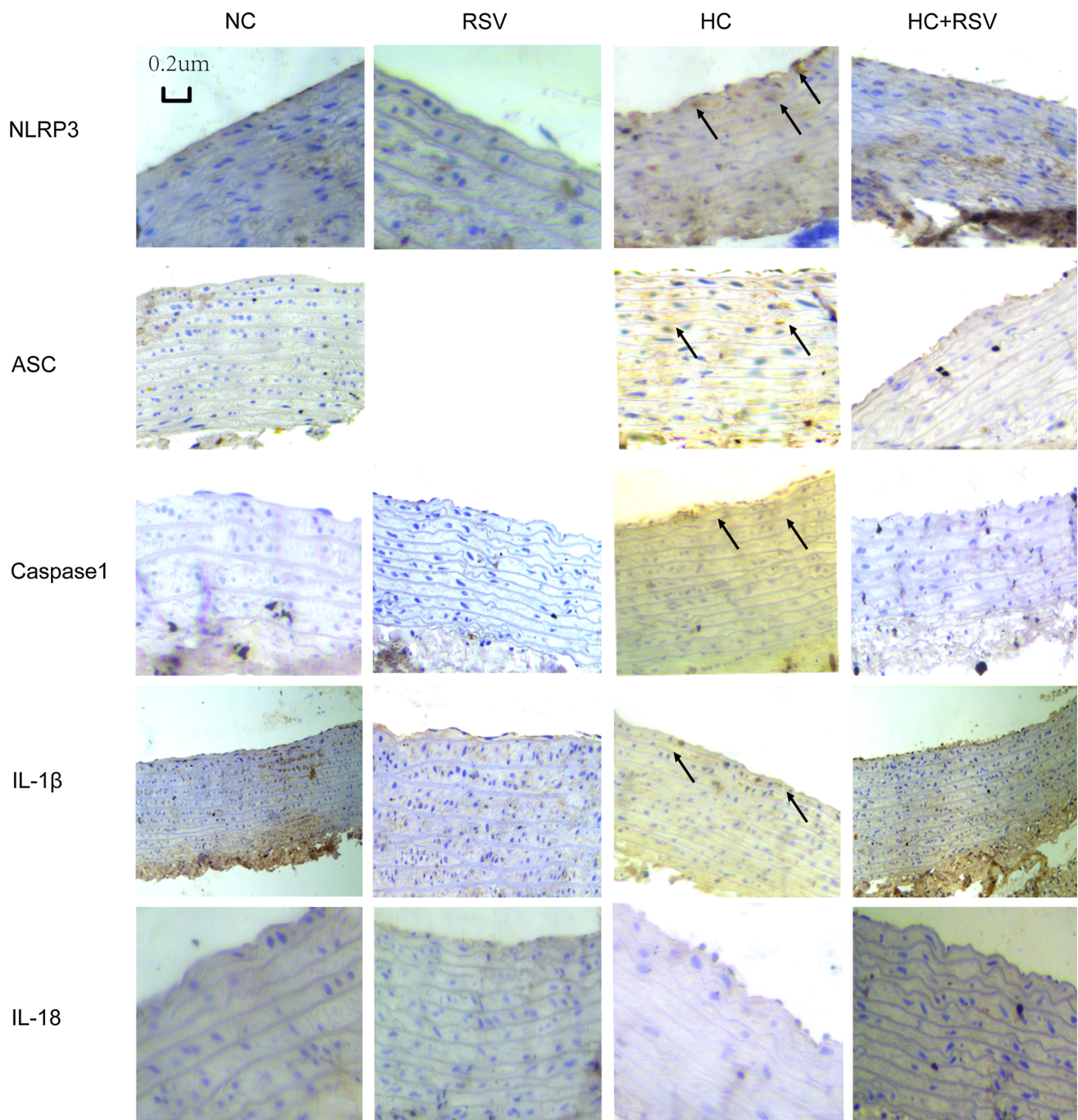
Fig. 7 RSV regulated the expression of NLRP3, ASC, and caspase-1, as well as the maturation of IL-1β and IL-18, in the aorta intima and media. Normal rats or rats with hypercholesterolemia combined with VD were administered with or without RSV (50 mg/kg/day) for 5 weeks. Animals were sacrificed, and the thoracic aorta samples were processed for immunohistochemistry. The expressions of NLRP3, ASC, and caspase-1, as well as the maturation of IL-1β and IL-18, were observed by immunohistochemical studies of the thoracic aorta. The *brown color* indicates immunoreactivity. *NC* normal; *HC+VD* hypercholesterolemia combined with vitamin D2; *RSV* resveratrol

the formation of cholesterol crystals and then inhibit inflammasome activation in hypercholesterolemia and VD rats.

Oxidative stress increases the production of NLRP3 and caspase-1, as well as the cleavage and release of pro-IL-1β

[14]. A hypercholesterol diet was used to induce hypercholesterolemia in our rat model. Hypercholesterolemia produces excess radicals that lead to oxidative stress, which is initiated in the presence of hydroxyl radicals, resulting in MDA production [18]. We also found decreased SOD and

Fig. 8 RSV inhibited the generation of inflammatory mediators in the vascular wall. Hypercholesterolemia combined with VD rats was fed with or without RSV (50 mg/ kg/day) for 5 weeks before the animals were sacrificed. **a** Thoracic aorta samples were extracted for total and nuclear proteins. The cytosolic fractions were used for Western blot analysis of LOX-1 MCP-1, ICAM-1, P38 MAPK, and p-P38 MAPK, whereas the nuclear fractions were used for NF-κB p65 in the thoracic aorta. **b** Total RNA from the thoracic artery of experimental rats and mRNA expression of LOX-1 MCP-1, ICAM-1, and P38 MAPK were determined by real-time RT-PCR. GAPDH was used as a standard housekeeping gene. The data are representative of three independent experiments. Results are expressed as the mean ± SEM for every three individual experiments. $*P < 0.05$, $**P < 0.01$, compared with NC rats; $\#P < 0.05$, $\#\#P < 0.01$, compared with HC rats
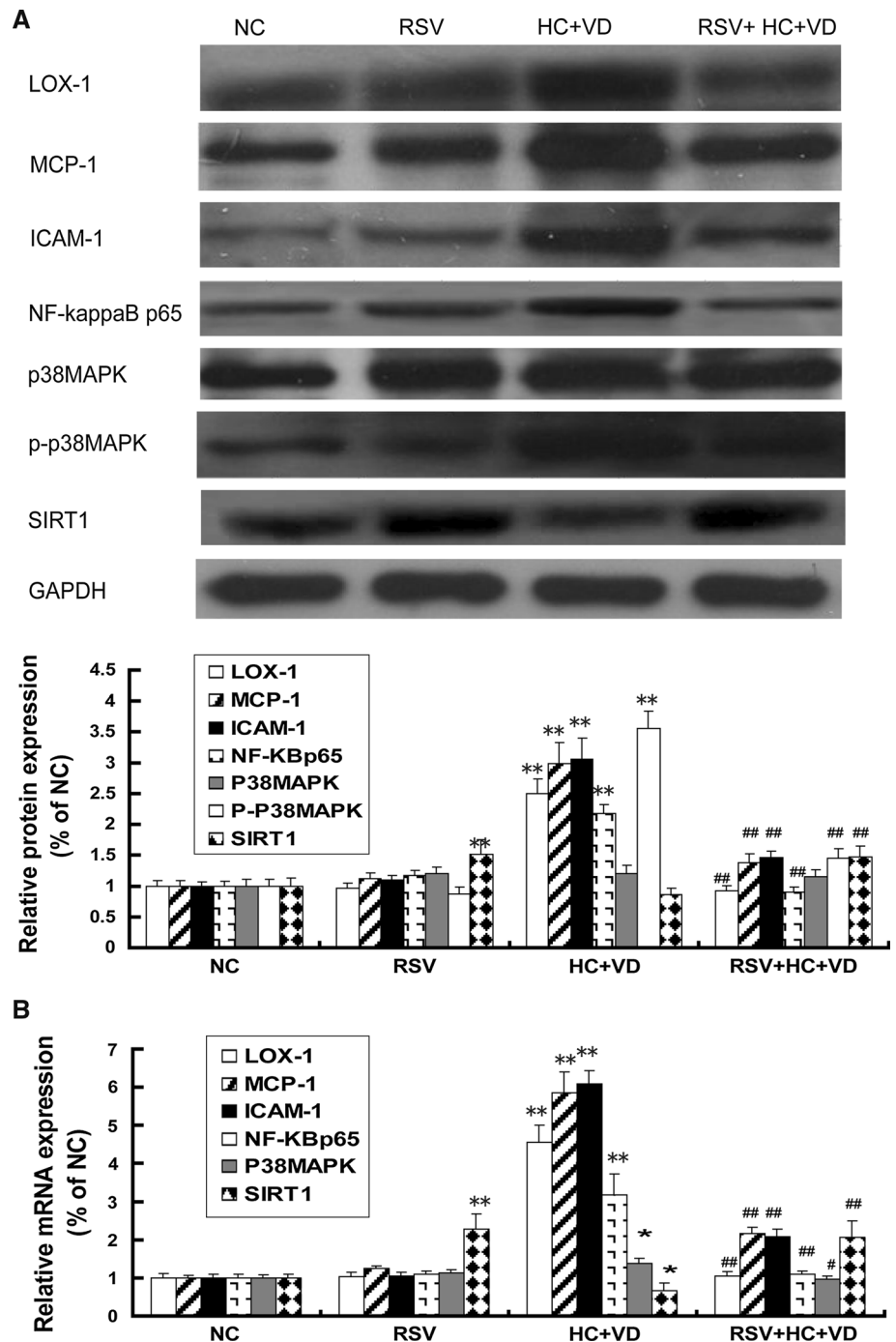
GPx activities and increased MDA content in our rat model. However, administration of RSV restored the balance between oxidants and antioxidants (increase in SOD and GPx, decrease in MDA). The function of RSV involves two antioxidants: non-enzymatic and enzymatic antioxidants. In non-enzymatic antioxidants, RSV is a natural polyphenolic compound; the polyphenolic structure of RSV makes it a ROS quencher and free radical scavenger [27]. In enzymatic antioxidants, RSV can regulate the expression and activity of various enzymes related to peroxidation and antioxidation. RSV inhibits NADH/NADPH oxidase enzyme activity and decreases ROS production. RSV regulates Nrf$_2$ expression and increases the expression of downstream targets (SOD and GPx) [28]. SOD, CAT, and GPx are susceptible to free radical attack and directly eliminate free radicals. Therefore, RSV inhibited NLRP3 activation via antioxidants and decreased ROS production.

In hypercholesterolemic rats, ox-LDL-binding LOX-1 enhanced the high expression of MCP, which transforms macrophages into a hypermigratory, pro-inflammatory phenotype [29]. Moreover, the damaged aorta produced TNF-α and IL-1β. MCP-1, TNF-α, and IL-1β induced the synthesis of adhesion molecules and inflammatory cytokines, such as ICAM-1, E-selectin, β2 integrin, vWF, and ET-1 [18, 30, 31]. These molecules induce adhesion between leukocytes and endothelial cells; leukocytes release oxygen free radicals and cytotoxic products, and cause further tissue damage [32]. Our data demonstrated that vascular injury was consistent with the increase in the protein expression levels of vWF, ICAM-1, and MCP-1, but RSV decreased the expression of vWF, ICAM-1, and MCP-1 in hypercholesterolemia and VD rats. We speculated that the vascular protective effects of RSV may be correlated with the diminution of the inflammatory response. Our results showed that RSV inhibited the expression and release of a vascular secretor by decreasing oxidative stress and lipid levels in hypercholesterolemia and VD rats.

Some studies speculated that the NF-κB and MAPK pathways are associated with inflammasome activation [8, 14]. Activation of the NF-κB pathway increases the transcription of the IL-1β gene encoding pro-IL-1β [33]. NLRP3 transcription is also dependent on the NF-κB pathway [15]. p38 MAPK phosphorylation significantly increased the mRNA expression of IL-1β and caspase-1, as well as the protein expression of pro-IL-1β [14]. In the present research, we obtained similar results with the aforementioned studies. Although we did not further study its mechanism, we observed the relative indices and found that the NF-κB and AMPK–SIRT1–PPAR signaling pathways were involved in the activation of inflammasome in rats with hypercholesterolemia and VD. Our results showed that the expression levels of mRNA and protein of NLRP3, ASC, caspase-1, IL-1β, NF-κB p65, and p38 MAPK were significantly elevated, whereas the mRNA and protein expression levels of SIRT1 were significantly decreased in hypercholesterolemia and VD rats. However, RSV downregulated the expression of the gene and proteins of NLRP3, ASC, caspase-1, IL-1β, NF-κB p65, and p38 MAPK but upregulated the gene and protein expression of SIRT1. These results indicated that the changes in NLRP3, ASC, caspase-1, and IL-1β were closely related to the changes in NF-κB p65 and p38 MAPK. RSV could affect the expression of IL-1β and NLRP3 by regulating the NF-κB p65 and p38 MAPK pathways. This trend was associated with the antioxidant effects of RSV because oxidative stress stimulates the expression of NF-κB p65 and p38 MAPK [28]. Furthermore, RSV inhibits NLRP3 activities by SIRT1 [34]. Given that RSV is a known SIRT1 activator, our results also confirmed that RSV increased the expression of SIRT1 in normal rats. SIRT1 suppressed the NF-κB pathway via the functional interaction between SIRT1 and NF-κB p65 [15]. Therefore, SIRT1 inhibited NLRP3 transcription by suppressing the NF-κB pathway.

In conclusion, our study proved that RSV affected the expression and activation of inflammasomes by hypolipidemia, antioxidation, and anti-inflammation, and decreased adhesion molecule expression. The P38 MAPK and NF-κB signaling pathways, as well as SIRT1 expression, were also involved in this process.

Conflict of interest The authors declare no conflicts of interest.

References

1. Ross R, Glomset JA. The pathogenesis of atherosclerosis (first of two parts). N Engl J Med. 1976;295:369–77.
2. Ross R, Glomset JA. The pathogenesis of atherosclerosis (second of two parts). N Eng J Med. 1976;295:420–5.
3. Ross R. The pathogenesis of atherosclerosis: a perspective for the 1990s. Nature. 1993;362:801–9.
4. Steinberg D. Atherogenesis in perspective: hypercholesterolemia and inflammation as partners in crime. Nat Med. 2002;8:1211–7.
5. Ross R. Atherosclerosis is an inflammatory disease. Am Heart J. 1999;138:S419–20.
6. Martinon F, Burns K, Tschopp J. The inflammasome: a molecular platform triggering activation of inflammatory caspases and processing of proIL-beta. Mol Cell. 2002;10:417–26.
7. Agostini L, Martinon F, Burns K, et al. NALP3 forms an IL-1beta-processing inflammasome with increased activity in Muckle-Wells autoinflammatory disorder. Immunity. 2004;20: 319–25.
8. Zheng X, Zhu S, Chang S, et al. Protective effects of chronic resveratrol treatment on vascular inflammatory injury in streptozotocin-induced type 2 diabetic rats: role of NF-kappa B signaling. Eur J Pharmacol. 2013;720:147–57.
9. Menu P, Vince JE. The NLRP3 inflammasome in health and disease: the good, the bad and the ugly. Clin Exp Immunol. 2011;166:1–15.
10. Schroder K, Zhou R, Tschopp J. The NLRP3 inflammasome: a sensor for metabolic danger? Science (NY). 2010;327:296–300.
11. De Nardo D, Latz E. NLRP3 inflammasomes link inflammation and metabolic disease. Trends Immunol. 2011;32:373–9.
12. Nakata R, Takahashi S, Inoue H. Recent advances in the study on resveratrol. Biol Pharm Bull. 2012;35:273–9.
13. Dong W, Wang X, Bi S, et al. Inhibitory effects of resveratrol on foam cell formation are mediated through monocyte chemotactic protein-1 and lipid metabolism-related proteins. Int J Mol Med. 2014;33(5):1161–8.
14. Huang TT, Lai HC, Chen YB, et al. cis-Resveratrol produces anti-inflammatory effects by inhibiting canonical and non-canonical inflammasomes in macrophages. Innate immun. 2013;20(7):735–50.
15. Fu Y, Wang Y, Du L, et al. Resveratrol inhibits ionising irradiation-induced inflammation in MSCs by activating SIRT1 and

limiting NLRP-3 inflammasome activation. Int J Mol Sci. 2013;14:14105–18.

16. Bennani-Kabchi N, Kehel L, el Bouayadi F, et al. New model of atherosclerosis in sand rats subjected to a high cholesterol diet and vitamin D2. Therapie. 1999;54:559–65.

17. Wen C, Yang X, Yan Z, et al. Nalp3 inflammasome is activated and required for vascular smooth muscle cell calcification. Int J Cardiol. 2013;168(3):2242–7.

18. Tang FT, Chen SRWu, Q X, et al. Hypercholesterolemia accelerates vascular calcification induced by excessive vitamin D via oxidative stress. Calcif Tissue Int. 2006;79(5):326–39.

19. Jiang HH, Liu Y, Lin GQ, Li YQ, xue xue bao Zhong nan da, xue ban Yi. Change of vWF, PAl-1 and t-PA in rats with hyperlipemia and its significance. Medical sciences. J Cent South Univ. 2008;n33:415–20.

20. Luo B, Li B, Wang W, et al. Rosuvastatin alleviates diabetic cardiomyopathy by inhibiting NLRP3. Inflammasome and MAPK pathways in a type 2 diabetes rat model. Cardiovasc Drugs Ther/Spons Int Soc Cardiovasc Pharmacother. 2014;28:33–43.

21. Weber A, Wasiliew P, Kracht M. Interleukin-1beta (IL-1beta) processing pathway. Sci Signal. 2010;3:105 (cm2).

22. Annabi B, Lord-Dufour S, Vezina A, Beliveau R. Resveratrol targeting of carcinogen-induced brain endothelial cell inflammation biomarkers MMP-9 and COX-2 is Sirt1-independent. Drug Target Insight. 2012;6:1–11.

23. Salado C, Olaso E, Gallot N, et al. Resveratrol prevents inflammation-dependent hepatic melanoma metastasis by inhibiting the secretion and effects of interleukin-18. J Transl Med. 2011;9:59.

24. Lu X, Kakkar V. Inflammasome and atherogenesis. Curr Pharm Des. 2014;20:108–24.

25. Deng Z, Liu B, Zhou J, et al. Effects of plasma very low density lipoprotein, low density lipoprotein and high density lipoprotein on platelet aggregation in endogenous hypertriglyceridemia. Medical science edition. J Sichuan Univ. 2003;34:704–7.

26. Chen M, Masaki T, Sawamura T. LOX-1, the receptor for oxidized low-density lipoprotein identified from endothelial cells: implications in endothelial dysfunction and atherosclerosis. Pharmacol Ther. 2002;95:89–100.

27. Vanaja K, Wahl MA, Bukarica L, Heinle H. Liposomes as carriers of the lipid soluble antioxidant resveratrol: evaluation of amelioration of oxidative stress by additional antioxidant vitamin. Life Sci. 2013;93:917–23.

28. Li H, Horke S, Forstermann U. Oxidative stress in vascular disease and its pharmacological prevention. Trends Pharmacol Sci. 2013;34:313–9.

29. Chen M, Nagase M, Fujita T, et al. Diabetes enhances lectin-like oxidized LDL receptor-1 (LOX-1) expression in the vascular endothelium: possible role of LOX-1 ligand and age. Biochem Biophys Res Commun. 2001;287:962–8.

30. Fan J, Watanabe T. Inflammatory reactions in the pathogenesis of atherosclerosis. J Atheroscler Thromb. 2003;10:63–71.

31. Liu X, Qu D, He F, et al. Effect of lycopene on the vascular endothelial function and expression of inflammatory agents in hyperhomocysteinemic rats. Asia Pac J Clin Nutr. 2007;16(Suppl 1):244–8.

32. Sena CM, Nunes E, Louro T, et al. Effects of alpha-lipoic acid on endothelial function in aged diabetic and high-fat fed rats. Br J Pharmacol. 2008;153:894–906.

33. Song R, Li WQ, Dou JL, et al. Resveratrol reduces inflammatory cytokines via inhibiting nuclear factor-kappaB and mitogen-activated protein kinase signal pathway in a rabbit atherosclerosis model. Zhonghua xin xue guan bing za zhi. 2013;41:866–9.

34. Galli M, Van Gool F, Leo O. Sirtuins and inflammation: friends or foes? Biochem Pharmacol. 2011;81:569–76.